ORGANOMETALLICS

Article

Cite This: *Organometallics* XXXX, XXX, XXX−XXX

pubs.acs.org/Organometallics

Monitoring Ligand Substitution in (Catalytically Active) Metal Complexes with Bodipy-Tagged Diimines and NHC Ligands

Oliver Halter, Jonas Spielmann, Yuki Kanai, and Herbert Plenio*

Organometallic Chemistry, TU Darmstadt, Alarich-Weiss-Str. 12, 64287 Darmstadt, Germany

Supporting Information

ABSTRACT: The reaction of 2,6-dimethyl-4-(Bodipy-8-yl)aniline with 1,4-dioxane-2,3-diol provides the respective diimine **3**, followed by ring closure with paraformaldehyde, resulting in the imidazolium salt **4**·HCl containing two fluorophores. The NHC metal complexes ([IrCl(cod)(**4**)], [Ir(cod)(**4**)(py)]-OTf, [$IrCl(CO)_2$(**4**)], [PdCl(allyl)(**4**)], [$PdCl_2$(Clpy)(**4**)], [AuCl(**4**)], and [NiCl(Cp)(**4**)]) were prepared. The complexes with (Au, Pd) are fluorescent. Weakly fluorescent complexes with Ir undergo fluorogenic reactions with CO and H_2. The oxidative addition of H_2 to [Ir(cod)(**4**)]OTf leads to a fluorescence gain of 8.2 and is suitable for the detection of hydrogen. Following activation of the diimine complex [$PdCl(CH_3)$(**3**)] with NaBArF, the formed [$Pd(CH_3)$(**3**)]BArF is a competent ethene polymerization catalyst. The addition of (pyridine, CH_3CN, CO) or olefins (ethene, 1-hexene, styrene) to the activated complex results in a pronounced increase in the fluorescence because of metal−ligand interactions and the modulation of photoinduced electron transfer quenching. The fluorescence response was used for the determination of the respective association constants with the donor molecules: 1-hexene (K = 9 L·mol^{-1}) and CH_3CN (K = 4 L·mol^{-1}); styrene is a poor ligand (K = 0.04 L·mol^{-1}). Based on the ν(CO) of the [$Mo(CO)_4$(**3**)] complex, the Bodipy-8-yl group is a moderately electron-withdrawing group, comparable to the Br substituent.

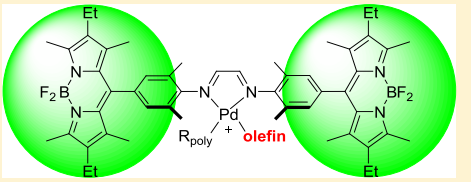

INTRODUCTION

The fluorescence light emitted from an excited fluorophore closely connected to a receptor unit can provide valuable information upon binding of a specific analyte by the host.[1] The fluorescence of the probe is modulated by the binding event, depending on the relative highest occupied molecular orbital (HOMO)−lowest unoccupied molecular orbital (LUMO) energies of the fluorophore and receptor.[2] This is compatible with a photoinduced electron transfer (PET) quenching mechanism.[3] Consequently, transition metal-based fluorescent receptors appear to be especially useful because the HOMO−LUMO energies of the metal can be manipulated by various elementary organometallic reactions (e.g., oxidative addition, ligand substitution, reductive elimination, insertion or migration, and redox reactions).[4] For a given fluorophore, changes in the electron density at the near-by transition metal lead to pronounced changes in the fluorescence, when the respective HOMO−LUMO energies of the fluorophore and metal are in the same range.[5] Consequently, fluorophores are useful reporter groups for (catalytically active) metal complexes. A catalyst is present in very small amounts relative to the substrates, whose conversion it is expected to catalyze, and it can be difficult to obtain useful information on this species by less sensitive spectroscopic techniques such as NMR.

The excellent detection sensitivity of fluorescence spectroscopy and the fact that only fluorescent molecules are observed can even provide information on individual fluorophore molecules. Based on this, fluorescence microscopy has become a useful tool for probing catalytic reactions.[1c] Ground-breaking single-molecule studies by Herten, Krämer et al. on copper complexes motivated organometallic chemists.[6] Blum et al. extensively established the use of fluorescence microscopy in transition-metal chemistry,[7] reporting in detail on various ruthenium-based olefin metathesis transformations.[8] Goldsmith et al. studied the initiation dynamics of surface-immobilized palladium-based cross-coupling catalysts.[9] ROMP reactions using fluorophore-tagged Grubbs−Hoveyda catalysts and the properties of the fluorescent polymer were investigated by Wöll, Mecking et al.[10]

However, this work is mainly limited to molecules deposited on a surface. We have decided to focus on ensemble measurements in solution because this better reflects the specific conditions met in homogeneous catalysis.[11] A highly useful fluorescent reporter group appears to be Bodipy (boron dipyrromethene, bdp).[12] It possesses many favorable properties (such as a high extinction coefficient, excellent fluorescence quantum yield, highly diverse functionalization chemistry, lipophilicity, and chemical stability),[13] which render it useful for applications in organometallic chemistry.

Fluorophore-tagged (mostly Bodipy) metal complexes are suitable for studying ligand substitution reactions in solution[14]—especially those involving catalytically active complexes (Scheme 1).[11,15] This provides information on the initiation of olefin metathesis catalysts (Scheme 1, a),[16] activating steps in gold-catalyzed transformation of alkynes (Scheme 1, b),[17] the fluorogenic detection of CO (Scheme 1,

Received: February 28, 2019

DOI: 10.1021/acs.organomet.9b00130
Organometallics XXXX, XXX, XXX−XXX

Scheme 1. Fluorogenic Reactions Involving Fluorophore-Tagged Transition-Metal Complexes[a]

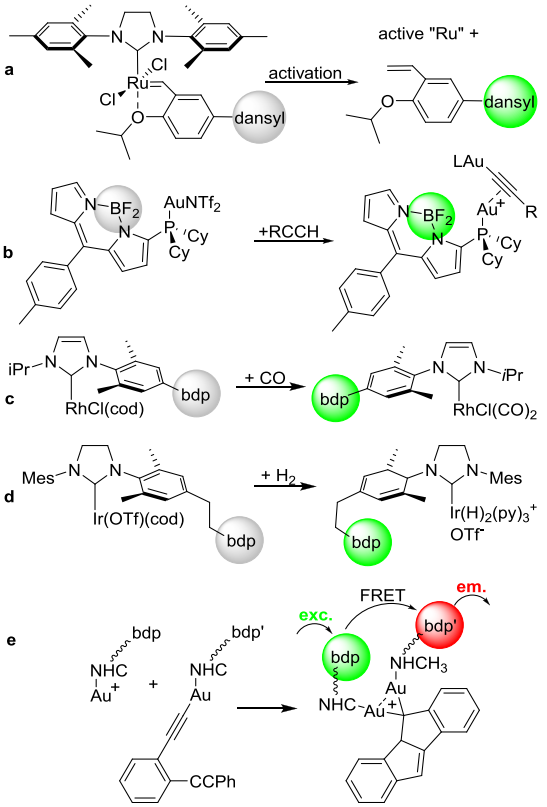

[a]bdp and bdp′ denote Bodipy groups with different peripheral substituents, bdp and bdp′ form a FRET pair, exc. = excitation, em. = emission, dansyl = 5-(dimethylamino)naphthalene-1-sulfonylamide, Tf = trifluoromethanesulfonate, L in AuL = the same Bdp-PCy$_2$ ligand.

c),[14a,18] the oxidative addition of H_2 to a Crabtree-like catalyst (Scheme 1, d),[19] or the formation of dimeric metal complexes in the course of gold-catalyzed cyclization reactions via the observation of a FRET signal (Scheme 1, e).[20] Bodipy-tagged olefin metathesis catalysts have also been employed to probe enyne-reactions or substrate−catalyst association.[21] Bodipy-substituted platinum complexes were employed in photocatalysis.[22]

Up until now, we have only synthesized ligands and the derived organometallic complexes containing one Bodipy per metal atom. However, certain metals like palladium and ruthenium tend to quench the fluorescence of the appended fluorophore very efficiently, resulting in "dark" complexes,[14a] while only a few tagged palladium complexes show modest fluorescence quantum yields.[23] We were hoping that ligands with two fluorophore molecules per palladium, would render brightly fluorescent complexes, in which the fluorophores are useful probes to study the rich catalytic chemistry of palladium complexes. Based on this concept, we want to report here on the facile synthesis of diimine and NHC ligands containing two Bodipy units, the derived metal complexes, and the fluorescence evolution during the interaction of olefins with Bodipy-tagged Brookhart-type catalysts[24] for ethene polymerization.

RESULTS AND DISCUSSION

Synthesis of Bodipy-Substituted Diimines and Azolium Salts. 4-Amino-3,5-dimethylbenzaldehyde[25] was synthesized from 2,6-dimethylaniline on a decagram scale via a Duff reaction[26] in good yields (Scheme 2). Bodipy **2** is available

Scheme 2. Synthesis of a Bodipy-Substituted Azolium Salt 4·HCl[a]

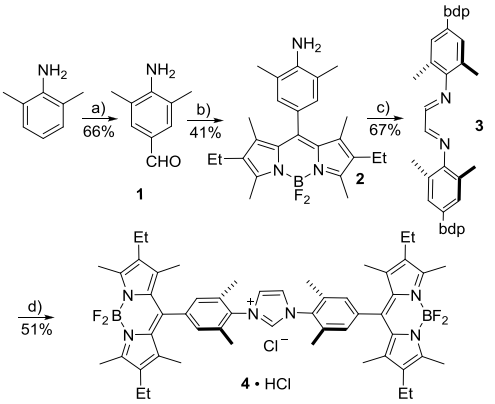

[a]Reagents and conditions: (a) 2,6 dimethylaniline, urotropine, AcOH, reflux 4 h; (b) 3-ethyl-2,4-dimethylpyrrole, CH_2Cl_2, 8 h, *para*-chloranil, 12 h, Et_3N, $BF_3{\cdot}OEt_2$; (c) 1,4-dioxane-2,3-diol and formic acid cat. and ethanol, reflux, 24 h; (d) paraformaldehyde, ethyl acetate, Me_3SiCl, 70 °C, 48 h.

using the established one-pot procedure utilizing aldehyde **1**. Protection of the amino group is not required because this group does not interfere with Bodipy synthesis. The procedure reported here is a significant improvement over the previously reported synthesis of **2**[27] and provides multigram amounts of Bodipy **2** in two steps from cheap commercially available materials. The formation of diimines from anilines with glyoxal is a very convenient reaction but tends to be less facile for the condensation of sterically demanding anilines with electron-withdrawing groups.[28] Therefore, the reaction of **2** leading to diimine **3** requires special precautions such as strictly anhydrous reaction conditions, freshly dried molecular sieve to remove the water formed in the reaction, and the use of 1,4-dioxane-2,3-diol as an anhydrous glyoxal surrogate.[29] Then, diimine **3** can be obtained in good yields of 67%. Cyclization of diimine **3** to the respective imidazolium salt according to the very useful, general Hintermann procedure provides the respective azolium salt **4**·HCl,[30] which serve as convenient precursors for NHC ligands.[31,32]

Synthesis of Metal Complexes with Diimine 3 and NHC 4 and Electronic Properties. Palladium complexes with diimine **3** were prepared according to the general procedure (Scheme 3)[33] by treating the respective metal source with diimine **3**. The two complexes [$PdCl_2$(**3**)] and [PdCl(Me)(**3**)] are formed in good yields. Following the activation with a Lewis acid, the latter complex forms an active ethene polymerization catalyst.[34] Diimine complex [Mo(CO)$_4$(**3**)] can be prepared by heating a tetrahydrofuran (THF) solution of **3** and $Mo(CO)_6$.[35]

Several new metal complexes utilizing the Bodipy-tagged NHC ligand **4** were prepared (Scheme 4) according to general literature procedures: [IrCl(cod)(**4**)],[36] [Ir(cod)(**4**)(py)$_2$]OTf,[19] [IrCl(CO)$_2$(**4**)],[36] [PdCl(allyl)(**4**)],[37] [$PdCl_2$(Clpy)-

DOI: 10.1021/acs.organomet.9b00130
Organometallics XXXX, XXX, XXX−XXX

Scheme 3. Synthesis of Bodipy-Diimine Metal Complexes[a]

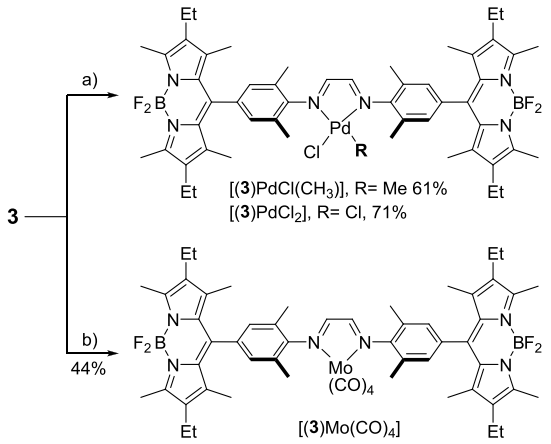

[a]Reagents and conditions: (a) $[PdCl(CH_3)(cod)]$ or $[PdCl_2(CH_3CN)_2]$, CH_2Cl_2, rt, N_2, 24 h, yield (R = CH_3) 61%, (R = Cl) 71%. (b) $Mo(CO)_6$, diimine **3**, THF, reflux, 18 h, yield 44%.

(**4**)], [AuCl(**4**)],[38] and [NiCl(Cp)(**4**)].[39] All complexes are air- and moisture-stable compounds.

The cyclic voltammogram of [IrCl(cod)(**4**)], namely, the Ir(I/II) redox potential, was determined to measure the donor properties of the NHC-ligand substituted with two electron-deficient Bodipy units.[28,40] The metal-centered quasi-reversible redox potential Ir(I/II) was shown to be $\Delta E_{1/2}$ = +0.93 V ($E_a - E_c$ = 80 mV). This redox potential is close to that of the related [IrCl(cod)(NHC)] complex with the highly electron-withdrawing $-SO_2$(tolyl) group ($\Delta E_{1/2}$ = +0.92 V).[28] Based on this, the Bodipy-8-yl substituent behaves like a highly electron-withdrawing group with a Hammett constant close to that of $\sigma_p(SO_2Et)$ = 0.77.[41] Bodipy itself is characterized by two (reversible) redox events corresponding to the oxidation and the reduction of the Bodipy, which depend on the nature of the substituents at the fluorophore.[42] The two redox potentials $\Delta E_{1/2}$(Bodipy/Bodipy$^+$) = +1.04 V ($E_a - E_c$ = 91 mV) and $\Delta E_{1/2}$(Bodipy/Bodipy$^-$) = −1.33 V ($E_a - E_c$ = 94 mV) are very close to those of 1,3,5,7-tetramethyl-2,6-diethyl-8-pentyl Bodipy ($\Delta E_{1/2}$ = −1.33, +1.02 V).[42] The orthogonal 8-aryl group in [IrCl(cod)(**4**)] has little influence on the redox potential. The pronounced electron-withdrawing effect of the Bodipy substituent on the redox potential of iridium is due to the π-face interaction of the *N*-aryl ring with the transition metal.[43]

In metal complexes of diimine **3** (Scheme 3), the *N*-aryl rings have a less favorable orientation relative to the metal center concerning potential π-face interactions. The electronic communication of the Bodipy substituents with the metal in the respective diimine complexes should thus be different. In order to establish this, Bodipy-substituted complex [Mo(CO)$_4$(**3**)] and the closely related diimine-Mo(CO)$_4$ complexes with 4-R = H or Br were studied.[35b] The determination of the donor properties of the diimine ligands via redox potentials of the respective metal complexes is not convenient because the diimines themselves are redox-active.[35b] Recently, Brenna et al. successfully employed infrared spectroscopy and ν(CO) for the determination of the donor properties of substituted phenanthrolines.[44] Concerning the related diimine, we decided to compare the respective [(diimine)Mo(CO)$_4$] complexes with 4-R = Bodipy ([Mo(CO)$_4$(**3**)]) and the closely related complexes with 4-R = H and 4-R = Br. The respective ν(CO) were determined to be 4-R = H 2008 cm^{-1}, 4-R = Br 2015 cm^{-1}, and 4-R = Bodipy (=[Mo(CO)$_4$(**3**)] (2015 cm^{-1})).[35a] In the absence of significant π-face interactions of the substituted *N*-aryl groups, the electronic influence of the Bodipy substituent on the metal is much weaker (comparable to a halide) than in the respective NHC complexes.

Fluorescence Properties. All new Bodipy-tagged compounds reported here show the same absorbance (λ_{max} = 526 nm) and emission maxima (λ_{em} = 538 nm). Obviously, none of the remote substituents in the different compounds has a

Scheme 4. Synthesis of NHC-Bodipy Metal Complexes[a]

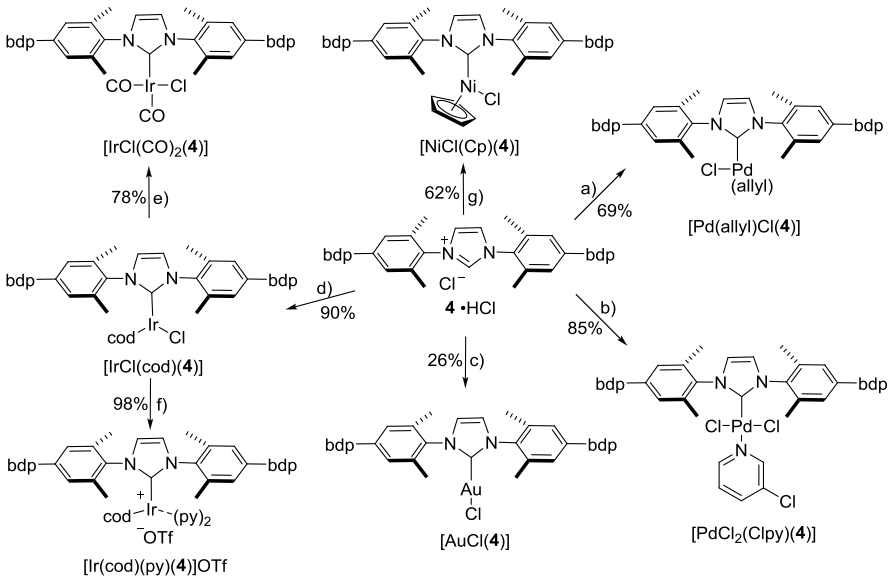

[a]Reagents and conditions: (a) **4**·HCl, $[PdCl(allyl)]_2$ and K_2CO_3 acetone, 60 °C, 4 h; (b) $PdCl_2$, **4**·HCl, Cl-pyridine solvent, K_2CO_3, 80 °C; 24 h; (c) $[AuCl(Me_2S)]$, **4**·HCl, K_2CO_3, 60 °C, acetone; (d) $[IrCl(cod)]_2$, CH_2Cl_2, 40 °C, **4**·HCl, Ag_2O; (e) [IrCl(cod)(**4**)], CO, 30 min, rt, CH_2Cl_2; (f) [IrCl(cod)(**4**)], [Ag(OTf)], CH_2Cl_2, rt, 2 h; (g) **4**·HCl, Cp_2Ni, THF, reflux, 24 h.

DOI: 10.1021/acs.organomet.9b00130
Organometallics XXXX, XXX, XXX−XXX

significant influence on the optical properties of the fluorophore. The fluorescence quantum yields of the newly synthesized compounds were determined (Table 1).[45] Diimine

Table 1. Fluorescence Quantum Yields for Diimine 3, Azolium Salt 4·HCl, and the Derived Metal Complexes in 1,2-Dichloroethane (c = 1.0 × 10^{-6} mol·L^{-1})[a]

compound	fluorescence quantum yield ϕ
3	0.49
[$PdCl_2$(**3**)]	0.003
[$PdCl(CH_3)$(**3**)]	0.06
[$Mo(CO)_4$(**3**)]	0.02
4·HCl	0.65
[IrCl(cod)(**4**)]	0.06
[$IrCl(CO)_2$(**4**)]	0.58
[Ir(cod)(py)(**4**)]OTf	0.05
[AuCl(**4**)]	0.67
[Pd(allyl)Cl(**4**)]	0.60
[$PdCl_2$(Clpy)(**4**)]	0.38
[NiCl(Cp)(**4**)]	0.03

[a]The absorbance and excitation maxima for all compounds are λ_{exc} = 526 nm and λ_{em} = 538 nm.

3 is characterized by a strong fluorescence, but for [$PdCl_2$(**3**)] and [$Mo(CO)_4$(**3**)], a pronounced quenching of the fluorescence is observed. Fortunately, [$PdCl(CH_3)$(**3**)] displays a decent fluorescence brightness (ϕ = 0.06).

Most of the NHC-metal complexes and the azolium salt itself display a strong fluorescence, namely, the complexes [$IrCl(CO)_2$(**4**)], [AuCl(**4**)], [Pd(allyl)Cl(**4**)], and [$PdCl_2$(Clpy)(**4**)] (Table 1). The strong fluorescence of the two palladium complexes is remarkable because a previously reported (NHC-Bodipy)Pd complex is characterized by a modest fluorescence quantum yields (ϕ = 0.03).[14a] This bright fluorescence offers chances for the monitoring cross-coupling reactions[46] or ligand exchange reactions[47] via fluorescence spectroscopy.[11] The most significant difference between [Pd(allyl)Cl(**4**)]/[$PdCl_2$(Clpy)(**4**)] and the previous Pd complexes is that the latter contains only a single Bodipy unit per palladium, which leads to very different fluorescence behavior. We expect that the quenching of two fluorophores by a single palladium should be less efficient than the interaction of one palladium with a single fluorophore. The proximity of the two Bodipy units does not seem to have a significant effect on the fluorescence properties because the conjugation path between the two dyes is interrupted.[48]

We have shown previously for related (NHC-Bodipy)gold complexes[5] that changes in the electron density at the metal center are very important for the fluorescence of the respective (Bodipy-NHC)metal complexes. Based on a systematic study of the fluorescence, it was concluded that PET quenching appears to be the dominant quenching mechanism in the various Bodipy-tagged transition-metal complexes.[5] Consequently, the systematic variation of the electron density at the transition metal allows the facile manipulation of the fluorescence.[18] Especially intermediate fluorescence quantum yields such as in [$PdCl(CH_3)$(**3**)] offer interesting analytic opportunities because a decrease or an increase in the electron density leads to corresponding changes in the fluorescence emission, both of which are easily observable. Such an approach was recently utilized in Bodipy-tagged phosphine–gold complexes to better understand the initial steps leading to gold-catalyzed alkyne transformations.[17]

Fluorogenic Reactions of (NHC)Ir Complexes with CO and H_2. The reaction of [IrCl(cod)(**4**)] with CO resulting in [$IrCl(CO)_2$(**4**)] is a fluorogenic reaction and leads to a pronounced increase in the fluorescence intensity (Figure 1)

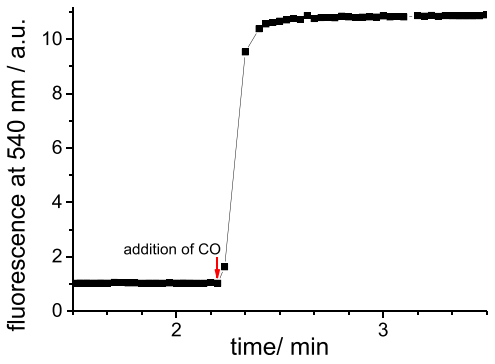

Figure 1. Fluorescence vs time plot for the reaction of [IrCl(cod)(**4**)] (c = 1.0 × 10^{-6} mol·L^{-1} in 1,2-dichloroethane) with CO (fluorescence gain = 11). The fluorescence of the initial complex is arbitrarily set to 1.0.

by a factor of 11. However, because the initial level of fluorescence is already high (for the reasons mentioned for the Pd complexes), the relative increase in the fluorescence is less pronounced than in complexes with a single Bodipy.[14a,18]

Previously, we had reported the first fluorogenic reaction involving H_2.[19] This is based on the oxidative addition of H_2 to a Crabtree catalyst-type complex. The complex studied then (Scheme 1d) is characterized by a relatively large distance between the fluorophore and transition-metal quencher, leading to lower efficiency of the PET quenching and based on this to a relatively high fluorescence level of the initial cationic iridium complex prior to the addition of H_2.

The obvious approach for a higher signal gain is to decrease the distance between the transition-metal quencher and the fluorophore. This should lead to a decreasing fluorescence level of the initial cationic [Ir(cod)(NHC-bdp)(py)] complex. Based on this criterion, the new complex [Ir(cod)(py)(**4**)]OTf might offer a stronger fluorescence response upon addition of H_2. The reaction with H_2 and the formation of the Ir(III) complex leads to a pronounced increase in the fluorescence by a factor of 8.2 (Figure 2). However, this gain is slightly smaller than the fluorescence gain of 11.7 observed previously.[19] Obviously, the effect of the closer vicinity of the Bodipy to the transition metal is overcompensated by the presence of two fluorophore molecules rather than just a single one. The obvious solution would be to synthesize a complex closely related to [Ir(cod)(py)(**4**)]OTf, but with only a single Bodipy unit. Unfortunately, this synthetic target so far has eluded all our synthetic efforts.

Reactions of [$PdCl(CH_3)$(3)] and [PdCl(allyl)(4)] with Thiolates. The interpretation of the fluorescence evolution in the various reactions of Bodipy-tagged metal complexes reported here is based on a predominately PET-based fluorescence quenching. This has been demonstrated previously for [(NHC-bdp)AuCl] complexes employing the chloride-to-thiolate substitution of RC_6H_4SH with electronically variable R groups[5] and should also be established for the complexes reported here.

DOI: 10.1021/acs.organomet.9b00130
Organometallics XXXX, XXX, XXX–XXX

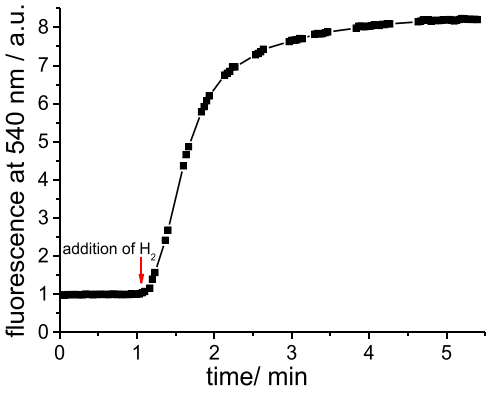

Figure 2. Fluorescence vs time plot for the reaction of [Ir(cod)(**4**)-(py)]OTf (c = 1.0 × 10^{-6} mol·L^{-1} in 1,2-dichloroethane) with H_2 (fluorescence gain = 8.2). The fluorescence of the initial complex is arbitrarily set to 1.0.

We first tested the reaction of [PdCl(CH_3)(**3**)] with thiolates. However, in the presence of an excess of PhSH, the diimine complex decomposes (as evidenced by NMR spectroscopy) to produce Pd-thiolates and an unknown diimine−thiol adduct. The reactions of [PdCl(allyl)(**4**)] with six different thiols RC_6H_4SH (R = CF_3, Cl, H, *t*Bu, OMe, NMe_2) lead to the clean formation of the respective [Pd(SR)(allyl)(**4**)] (evidenced by NMR spectroscopy). Closely related palladium-thiolates with a phosphine instead of the NHC ligand are known.[49] Electron-deficient thiols react very fast, while the electron-rich thiols are converted progressively slower. It appears that the acidity of the thiol is important for a fast reaction with the metal complex.

Replacing chloride by electron-rich thiolates leads to a significant decrease in the fluorescence because of the formation of the electron-rich Pd-thiolates (Figure 3). This

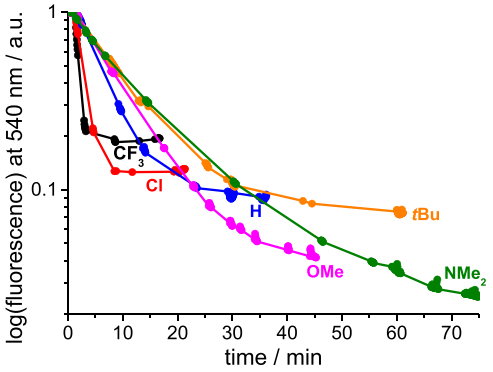

Figure 3. log fluorescence vs time plot for the reactions of [PdCl(allyl)(**4**)] (c = 1.0 × 10^{-6} mol·L^{-1}) with thiolates RC_6H_4SH (R = CF_3, Cl, H, *t*Bu, OMe, NMe_2) (1000 equiv) in the presence of Hünig base (100 equiv). The fluorescence of the initial [PdCl(allyl)-(**4**)] is arbitrarily set to 1.0.

decrease depends on the nature of R and is more pronounced for electron-rich thiols than for the electron-deficient thiols. The final fluorescence intensities of the respective thiolates are correlated with the Hammett constants[41] of the respective R groups (Hammett plot, Figure S52, Supporting Information). In conclusion, our experiments provide convincing arguments for the importance of PET quenching in the palladium complexes studied here—similar to the gold thiolates reported previously.[5] Based on the observation that an increase in the electron density leads to a decrease in the fluorescence, an acceptor PET mechanism likely is the dominant quenching pathway in the NHC metal complexes reported here.[5]

Interaction of Ligands with [Pd(Me)(3)]BArF. The activation of [PdCl(Me)(**3**)][50] with NaBArF (sodium tetrakis-(3,5-bis(trifluoromethyl)phenyl)borate)[51] generates [Pd(Me)-(**3**)]BArF, in which the strongly coordinating chloride is replaced by the very weakly coordinating $BArF^-$ counterion. The activation of the palladium complex leads to the in situ formation of the cationic complex [Pd(Me)(**3**)]$^+BArF^-$ resulting in a minor dip in the fluorescence from 1.0 to 0.8 (Figure 4, inset). This emission change is comparable to the ca.

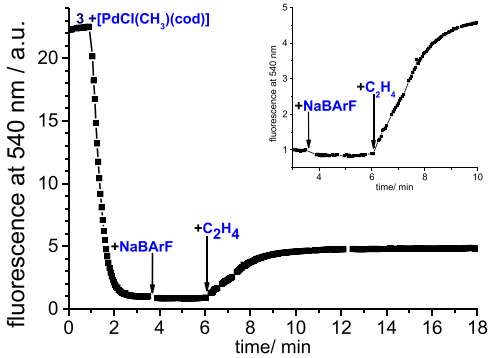

Figure 4. Fluorescence vs time plot for the reaction of diimine **3** (c = 1.0 × 10^{-6} mol·L^{-1} in 1,2-dichloroethane) with [PdCl(CH_3)(cod)] followed by the activation with NaBArF (see inset for magnified view), followed by the addition of ethene and polymerization. The fluorescence of [PdCl(CH_3)(**3**)] is arbitrarily set to 1.0.

25% decrease in fluorescence upon substitution of a coordinating chloride in [AuCl(Bodipy-PCy_2)] with a weakly coordinating triflate ion.[17] Next, the coordination of donor molecules by the cationic palladium complex can be followed via the fluorescence evolution of the Bodipy tag. In general, the addition of ligands results in a significant increase in the fluorescence intensity. First, the reaction of two strong ligands L = pyridine and CO with the cationic palladium complex was tested (Scheme 5). In both reactions, the addition of a large excess ligand to the cationic palladium led to the fast formation of the respective complexes [Pd(Me)(**3**)(L)]BArF. For L = py, the fluorescence increases 12-fold (gain = 44), for L = CO (gain = 6). The closely related [Pd(Me)(diimine)(CO)]BArF complexes are well established in the literature.[52]

It was tried to determine the equilibrium constant of the pyridine complex by lowering the amount of added pyridine. However, at c([Pd(Me)(**3**)]BArF) = 1.0 × 10^{-6} mol·L^{-1}, even 0.1 μL of pyridine led to the nearly quantitative formation of the respective pyridine complex. Further lowering the amount of pyridine results in very long reaction times. Based on this, the equilibrium constant K(py) was estimated to be larger than 10^5 L·mol^{-1}. CH_3CN is a much weaker ligand toward cationic late transition metals than CO and pyridine[53] and its binding strength toward the cationic diimine Pd complexes was previously found to be in the same range as that of simple alkenes.[54] The use of labile ligands in such complexes is important because in order to form highly active polymerization catalysts, the respective donor ligand should be efficiently replaced by the olefin to be polymerized. The addition of CH_3CN to in situ generated [Pd(CH_3)(**3**)]BArF

DOI: 10.1021/acs.organomet.9b00130
Organometallics XXXX, XXX, XXX−XXX

Scheme 5. Association of Ligand L with Cationic Complex [Pd(Me)(3)]$^+$BArF$^-$ (L = py, CH_3CN, Et_2O or Olefins such as Ethene, 1-Hexene, Styrene)

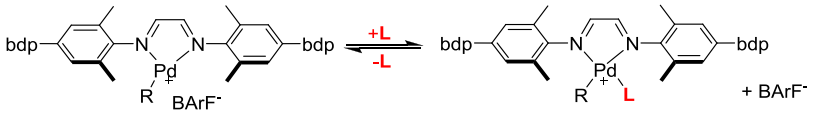

leads to an up to 50-fold increase in the fluorescence. Saturation, because of the nearly quantitative formation of [Pd(Me)(**3**)(CH_3CN)]BArF, is reached after addition of ca. 10^5 equiv of CH_3CN. The quantitative evaluation of the titration data via the Scatchard method[55] provides the respective equilibrium constant $K(CH_3CN)$ = 4.2 L·mol^{-1}. The stability constants for THF (K = 1.7 L·mol^{-1}) and Et_2O (K = 1.1 L·mol^{-1}) were determined accordingly and are weaker than those of CH_3CN.[56] This explains why the Et_2O adduct of the nontagged analogue of complex [Pd(Me)(**3**)-(Et_2O)]BArF was reported to be highly labile.[54]

Fluorescence Evolution of [Pd(Me)(3)]BArF during the Reaction with Olefins. The interaction of olefins with the cationic palladium complex is more interesting than those of the simple ligands (CO, py or CH_3CN) because cationic [Pd(CH_3)(diimine)]$^+$ species are a competent polymerization catalyst.[24,34a,57] The sequence of reactions leading to the polymerization of ethene with [Pd(Me)(**3**)]BArF can be monitored by recording the fluorescence of the reaction of Bodipy-tagged diimine ligand **3** and [PdCl(Me)(cod)] (Figure 4) followed by the activation with NaBArF and followed by ethene addition. To a solution of diimine **3** (c = 1.0 × 10^{-6} mol·L^{-1}) in 1,2-dichloroethane was added [PdCl(CH_3)(cod)], leading to the rapid formation of [PdCl(Me)(**3**)]. This reaction is accompanied by a pronounced decrease in the fluorescence level from 22.5 for the diimine to 1.0 for [PdCl(Me)(**3**)]. The reaction with NaBArF leads to the modest decrease in fluorescence (see previous section) and the formation of [Pd(Me)(**3**)]BArF. The addition of ethene to this activated complex results in a pronounced increase in the fluorescence to 4.9. Adding more ethene after 30 min reaction time (re-saturation) has no effect on the fluorescence. The change in the fluorescence should initially be due to the formation of [Pd(Me)(**3**)(ethene)]BArF. At the same time, the activated complex is a polymerization catalyst and the insertion of ethene into the Pd–alkyl bond leads to the formation of the respective complexes [Pd((C_2H_4)$_n$Me)(**3**)-(ethene)]$^+$. Because such complexes are known to be the resting states in palladium-catalyzed ethene polymerization reactions, the fluorescence is dominated by those species.[24,54,58] All complexes with n = 0 and n > 0 are expected to display the same fluorescence properties because any changes in the remote alkyl substitution should be negligible concerning the PET quenching of the fluorophore.

The equilibrium constant determined via this approach should correspond to the equilibrium constant for the simple reaction, [Pd(Me)(**3**)]BArF + olefin = [Pd(Me)(**3**)(olefin)]$^+$ + BArF$^-$, under the following assumptions: the different insertion products [Pd((C_2H_4)$_n$Me)(**3**)(ethene)]$^+$ have the same affinity to ethene independent of the value of n. This should hold true in a good approximation for low degrees of polymerization. Furthermore, c(ethene) should be virtually constant throughout the reaction. This condition is met because the olefin is present in ca. 10^5-fold excess relative to the cationic palladium species. Furthermore, the re-saturation with ethene has no effect on the fluorescence. Another supportive observation is that the fluorescence–time trace reaches a constant value after ca. 5 min exposure to ethene. Because of the extremely small amounts of the palladium complex contained in the fluorescence cuvette (ca. 2.0 × 10^{-9} mol), direct proof of the polymerization reaction in the cuvette could not be obtained. In separate experiments on a larger scale (under otherwise similar conditions), it was shown that the Bodipy-tagged complex [PdCl(Me)(**3**)] activated with NaBArF is a competent ethene polymerization catalyst, leading to the formation of polyethene (Supporting Information).

Probably the most interesting step in the sequence of reactions leading to the polymerization of ethene is the association of an olefin with the activated palladium complex. This step can be followed conveniently by fluorescence spectroscopy because it is associated with a pronounced change in the fluorescence.

Because ethene is a gas under ambient conditions, control over the concentration of this gas below the saturation level in the cuvette solution is experimentally difficult.[59] However, the concentration of liquid olefins in the reaction mixture can be adjusted precisely and consequently reactions with 1-hexene, styrene, and methacrylate were studied. The stepwise addition of 1-hexene to a solution of [Pd(CH_3)(**3**)]BArF leads to a pronounced increase in the fluorescence (Figure 5) corresponding to the formation of [Pd(CH_3)(**3**)(1-hexene)]BArF and of the respective insertion products. The reaction of the olefin with the activated palladium complex appears to be an equilibrium reaction. The calculated equilibrium constant is K(1-hexene) = 9 L·mol^{-1}. Closely related complexes (without the Bodipy tag) can polymerize 1-hexene—albeit at a much slower rate than ethene.[60] However, in the fluorescence experiments, we do not observe any significant polymer formation with 1-hexene. The respective association constant for styrene were determined in the same way: K(styrene) = 0.04 L·mol^{-1}.[61] Methacrylate was also tested, but the metal

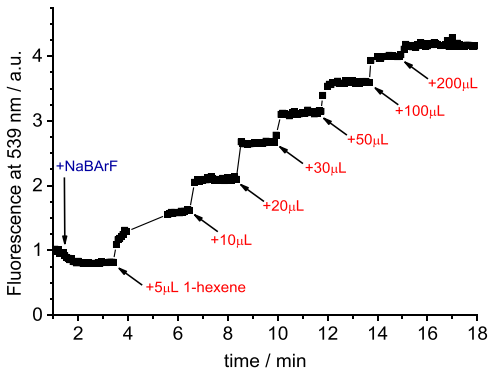

Figure 5. Fluorescence intensity vs time plot for the reactions of [PdCl(Me)(**3**)] (c = 1.0 × 10^{-6} M) in 1,2-dichloroethane (2 mL) with NaBArF (100 equiv) followed by addition of 1-hexene; 1 µL corresponds to 4000 equiv of 1-hexene. The fluorescence of [PdCl(Me)(**3**)]is arbitrarily set to 1.0.

DOI: 10.1021/acs.organomet.9b00130
Organometallics XXXX, XXX, XXX–XXX

binding is even weaker than styrene and an association constant could not be determined. Based on our fluorescence experiments, the binding of 1-hexene is approx. twice as strong as that of CH_3CN, which is compatible with literature data.[54,62] The stability constants for propene and PhCN determined by Kurosawa et al. for cationic cyclopentadienyl-palladium complexes also are almost the same.[63]

Following the activation of [PdCl(CH_3)(**3**)] with NaBArF, the coordination of donor ligands leads to a pronounced increase in the fluorescence as a consequence of the increased electron density at the "cationic" palladium. This is indicative of a donor-PET quenching mechanism for the diimine complexes as opposed to an acceptor-PET reported for the NHC metal complexes.[64] With a view to the much weaker donicity of diimines compared to NHC ligands, this is plausible.[40b]

CONCLUSIONS

Based on the facile synthesis of Bodipy-substituted aniline **2**, numerous transition-metal NHC and diimine complexes containing two Bodipy fluorophores were synthesized and the variation of the fluorescence of the appended fluorophore during various ligand substitution reactions monitored. In NHC(**4**)-metal complexes, the increase of electron density on the metal leads to a decrease in the fluorescence. In the related diimine(**3**)-metal complexes, similar reactions led to an increase in the fluorescence intensity. This is indicative of acceptor-PET quenching for the former and donor-PET for the latter metal complexes. The changes in the fluorescence are analytically useful for monitoring chemical transformations at the metal center in the course of catalytic transformations at catalytically relevant concentrations of the respective metal complex. The activated [Pd(Me)(**3**)]BArF coordinates donor solvents and olefins. Changes in the fluorescence enable the determination of the respective association constants for the metal–ligand interaction. The binding of CO and pyridine to the cationic palladium complex is much stronger than that of ligands such as 1-hexene > CH_3CN > THF > Et_2O. Styrene and methacrylate are very weak ligands. This work has demonstrated the usefulness of fluorescence spectroscopy as an analytic tool in fluorophore-tagged metal complexes, leading to a better understanding of the chemistry at the metal center in a catalytically relevant concentration range.

EXPERIMENTAL SECTION

General Experiment. All reactions involving transition-metal complexes were conducted in oven-dried glassware. Reactions were performed in Schlenk flasks under a positive pressure of argon or nitrogen. The flasks were fitted with rubber septa, and gas-tight syringes with stainless steel needles or double-cannula were used to transfer air- and moisture-sensitive liquids.

Materials. All chemicals were purchased as reagent grade from commercial suppliers and used without further purification, unless otherwise noted. THF was dried under sodium and distilled under argon atmosphere. 1,2-Dichloroethane was dried over CaH_2. All solvents for synthesis were stored over molecular sieves. Solvents stored over molecular sieve are only suitable for fluorescence measurements after careful filtrations because small amounts of molecular sieve dust can lead to high levels of scattered excitation light. Preparative chromatography was performed using Merck silica 60 (0.063–0.2 mm).

Instrumentations. The chemical shifts are given in parts per million on the delta scale (δ) and are referenced to tetramethylsilane (^{1}H, ^{13}C NMR = 0.0 ppm), the residual peaks of $CDCl_3$ (^{1}H NMR = 7.26 ppm, ^{13}C NMR = 77.23 ppm), dimethyl sulfoxide (^{1}H NMR = 2.50 ppm, ^{13}C NMR = 39.51 ppm), CD_2Cl_2 (^{1}H NMR = 5.32 ppm), or hexafluorobenzene (^{19}F NMR = −164.90 ppm). Mass spectra were recorded on the Finnigan MAT95 spectrometer using electron ionization. UV–vis spectra were recorded on the Analytik Jena SPECORD 600 UV–vis spectrometer, and fluorescence spectra were recorded on a J&M TIDAS S700/CCD UV/NIR 2098 spectrometer combined with a J&M TIDAS LSM monochromator with 75 W xenon light source and thermo-controlled cuvette holder. Samples for emission and absorption measurements were contained in a 1 cm × 1 cm quartz cuvette (Hellma Analytics, lot. 111-10-40). Cyclic voltammetry was performed using a standard electrochemical instrumentation consisted of an EG&G 273A-2 potentiostat–galvanostat. A three-electrode configuration was employed. The working electrode was a Pt disk (diameter 1 mm) sealed in soft glass with a Pt wire as a counter electrode. The pseudo reference electrode was a Ag wire. Potentials were calibrated internally against the formal potential of ferrocene (+0.46 V vs Ag/AgCl) or octamethylferrocene (−0.01 V vs Ag/AgCl). All cyclic voltammograms were recorded in dry CH_2Cl_2 under an atmosphere of argon, supporting electrolyte N*n*Bu_4PF_6 (c = 0.1 mol/L).

Synthesis of 4-Amino-3,5-dimethylbenzaldehyde 1. In a 1 L round-bottom flask, 2,6-dimethylaniline (20.52 g, 0.1693 mol, 1 equiv) and urotropine (47.4 g, 0.338 mol, 2 equiv) were dissolved in a mixture (600 mL) of AcOH/H_2O (3:1) and heated to reflux for 4 h. The mixture was allowed to cool down to room temperature. Next, H_2O (100 mL) was added, and the reaction mixture was extracted four times with CH_2Cl_2. The combined organic layers were washed with saturated aq. $NaHCO_3$ solution and brine. The organic solution was dried over $MgSO_4$ and filtered off. The volatiles of the filtrate were evaporated under reduced pressure. The remaining residue was carefully purified by column chromatography (Cy/EA = 1:1). The product is a yellowish oily solid 16.4 g (0.110 mol, 66%).

^{1}H NMR ($CDCl_3$, 500 MHz): δ 9.71 (s, 1H, CH), 7.47 (s, 2H, CH), 4.21 (s, 2H, NH_2), 2.21 (s, 6H, CH_3). ^{13}C NMR ($CDCl_3$, 126 MHz): δ 191.05, 149.31, 130.93, 127.02, 120.96, 14.46.

Synthesis of Bodipy-Aniline 2. 3-Ethyl-2,4-dimethylpyrrole (2.45 mL 18.09 mmol, 2.05 equiv) and 4-amino-3,5-dimethylbenzaldehyde (8.83 mmol, 1 equiv) were dissolved in 100 mL of CH_2Cl_2 containing a catalytic amount of trifluoroacetyl (12 drops). The resulting mixture was stirred for 9 h at room temperature under a N_2 atmosphere. *para*-Chloranil (3.91 g, 15.89 mmol, 1.8 equiv) was added to the reaction mixture, while cooling the flask because of the exothermic reaction. The dark suspension was stirred at room temperature for 12 h, and then, Et_3N (12.41 mL, 88.29 mmol, 10 equiv) added. Stirring was continued for 2 h at room temperature and next $BF_3{\cdot}OEt_2$ (16.34 mL, 132.42 mmol, 15 equiv) was added to the stirred solution. After 3 h, the reaction mixture was transferred to a 2 L separation funnel, washed with saturated $NaHCO_3$ solution (1.5 L), and extracted with CH_2Cl_2 (1 L). The organic phase was dried over magnesium sulfate. The volatiles were removed under reduced pressure, and the remaining residue was purified by column chromatography (Cy/EA 4:1) to obtain the desired dark reddish product (1.69 g, 4.00 mmol, 41%).

^{1}H NMR ($CDCl_3$, 500 MHz): δ 6.81 (s, 2H, CH), 3.73 (s, 2H, NH_2), 2.52 (s, 6H, CH_3), 2.30 (q, 4H, CH_2), 2.22 (s, 6H, CH_3), 1.37 (s, 6H, CH_3), 0.99 (t, 6H, CH_3). ^{13}C NMR ($CDCl_3$, 126 MHz): δ 153.03, 143.14, 141.75, 138.67, 132.42, 131.53, 128.05, 125.08, 122.33, 17.67, 17.23, 14.77, 12.57, 12.16. ^{19}F NMR ($CDCl_3$, 471 MHz): δ −148.84 (q, 4F, BF_2). ESI HR-MS m/z: calcd for $C_{25}H_{33}BF_2N_3$ $[M + H]^+$, 424.27301; found, 424.27370.

Synthesis of Diimine 3. An oven-dried Soxhlet extractor with a Dimroth condenser connected to a 100 mL Schlenk flask was used for the synthesis of compound **3**. The Soxhlet extractor was charged with 30 g of carefully dried 3 Å-molecular sieve (100 °C for 2 d at 0.1 mbar, followed by 300 °C for 30 min at 0.1 mbar). Bodipy-aniline **2** (1.97 g, 4.65 mmol, 2.1 equiv), 1,4-dioxan-2,3-diol (262.3 mg, 2.21 mmol, 1 equiv), and 30 drops formic acid were suspended in dry ethanol (60 mL). The reaction mixture was heated to 110 °C for 48 h. Precipitation of the desired diimine **3** begins after ca. 1 h of reaction

DOI: 10.1021/acs.organomet.9b00130
Organometallics XXXX, XXX, XXX–XXX

time. After the 48 h, the reaction mixture was cooled to −10 °C, and the precipitate was filtered off. The residue was washed with cold abs. ethanol (6 mL) and *n*-pentane (6 mL). Compound **3** is an orange solid (1.35 g, 1.56 mmol, 67%).

^{1}H NMR ($CDCl_3$, 500 MHz): δ 8.22 (s, 2H, CH), 7.04 (s, 4H, CH), 2.54 (s, 12H, CH_3), 2.33 (q, 8H, CH_2), 2.26 (s, 12H, CH_3), 1.42 (s, 12H, CH_3), 1.01 (t, 12H, CH_3). ^{13}C NMR ($CDCl_3$, 126 MHz): δ 163.84, 153.33, 150.33, 140.18, 138.40, 132.55, 131.05, 128.30, 127.59, 18.38, 17.24, 14.76, 12.64, 12.10. ^{19}F NMR ($CDCl_3$, 471 MHz): δ −148.84 (m, 4F, BF_2). ESI HR-MS *m*/*z*: calcd for $C_{52}H_{63}B_2F_4N_6$ $[M]^+$, 869.52310; found, 869.52447.

Synthesis of Imidazolium Salt 4·HCl. A 25 mL Schlenk flask was charged with diimine **3** (300 mg, 0.345 mmol, 1 equiv), paraformaldehyde (10.5 mg, 0.349 mmol, 1.01 equiv), Me_3SiCl (37.6 mg, 44 μL, 0.347 mmol, 1 equiv), and abs. EtOAc (12 mL). The reaction mixture was heated to 70 °C for 48 h. The suspension was cooled to room temperature, and the solvent was removed under reduced pressure. The residue was purified by column chromatography ($CHCl_3$/MeOH 10:1). The desired product is an orange solid (163 mg, 0.178 mmol, 51%).

^{1}H NMR (300 MHz, $CDCl_3$): δ 11.97 (s, 1H, CH), 7.64 (s, 2H, CH), 7.28 (s, 4H, CH), 2.53 (s, 12H, CH_3), 2.37 (s, 12H, CH_3), 2.31 (t, 8H, CH_2), 1.47 (s, 6H, CH_3), 1.41 (s, 6H, CH_3), 1.01 (t, 6H, CH_3), 0.97 (t, 6H, CH_3). ^{13}C NMR (126 MHz, $CDCl_3$): δ 155.66, 153.54, 141.66, 139.79, 139.48, 137.49, 136.88, 135.85, 133.89, 133.46, 132.85, 130.83, 129.96, 129.65, 124.13, 77.16, 18.08, 17.20, 17.13, 14.75, 14.60, 13.06, 12.73, 12.58, 12.28. ^{19}F NMR (471 MHz, $CDCl_3$): δ −148.69, −148.89 (m, 4F, BF_2). ESI HR-MS *m*/*z*: calcd for $C_{53}H_{63}B_2F_4N_6$ $[M]^+$, 881.52310; found, 881.52488.

Synthesis of [IrCl(cod)(4)]. To a Schlenk tube (10 mL) equipped with a stirring bar and **4**·HCl (50 mg, 0.0545 mmol, 1 equiv) were added Ag_2O (6.3 mg, 0.0273 mmol, 0.5 equiv) and CH_2Cl_2 (5 mL). The reaction mixture was heated to 40 °C for 3 h, and the solvent was removed under reduced pressure. The remaining residue was suspended in toluene. Next, $[IrCl(cod)]_2$ (17.3 mg, 0.0273 mmol, 0.5 equiv) was added to the suspension and allowed to react for 4 h at 100 °C. The solution was filtered through Celite, evaporated, and purified by chromatography (EA). The volatiles were removed to give product [IrCl(cod)(**4**)] as an orange solid (60 mg, 0.0593 mmol, 90%).

^{1}H NMR ($CDCl_3$, 500 MHz): δ 7.19 (s, 4H, CH), 6.98 (s, 2H, CH), 4.29 (s, 2H, CH), 3.13 (s, 2H, CH), 2.56 (s, 6H, CH_3), 2.55 (s, 6H, CH_3), 2.46 (s, 6H, CH_3), 2.34 (m, 14H, CH_3/CH_2), 1.90−1.80 (m, 4H, CH_2), 1.67 (s, 6H, CH_3), 1.61−1.46 (m, 4H, CH_2), 1.36 (s, 6H, CH_3), 1.025 (t, 6H, CH_3), 1.015 (t, 6H, CH_3). ^{13}C NMR ($CDCl_3$, 126 MHz): δ 180.51, 154.82, 153.48, 139.32, 139.11, 137.50, 136.83, 133.28, 132.83, 130.76, 130.63, 129.12, 127.94, 124.10, 84.44, 77.42, 77.16, 76.91, 51.74, 33.74, 29.19, 19.99, 18.47, 17.28, 17.24, 14.78, 13.27, 12.75, 12.63, 11.85. ^{19}F NMR ($CDCl_3$, 471 MHz): δ −148.90 (m, 4F, BF_2). ESI HR-MS *m*/*z*: calcd for $C_{61}H_{74}IrB_2F_4N_6$ $[M]^+$, 1181.57210; found, 1181.57433.

Synthesis of [Ir(cod)(4)(py)]OTf. To a flame-dried Schlenk flask containing [IrCl(cod)(**4**)] (41.2 mg, 33.9 mmol, 1 equiv) was added CH_2Cl_2 (5 mL), followed by pyridine (4.1 μL, 4.0 mg, 50.8 μmol, 1.5 equiv) and $[Ag(CF_3SO_3)]$ (8.7 mg, 33.9 μmol, 1 equiv). The reaction mixture was stirred for 1 h and then filtered through a Celite plug. The filtrate was evaporated under reduced pressure. The solid residue was dissolved in a minimum amount of CH_2Cl_2 and precipitated from diethyl ether. The precipitate was collected by filtration and dried under vacuum. The product was obtained as an orange microcrystalline solid (46.8 mg, 33 μmol, yield 98%).

^{1}H NMR (500 MHz, $CDCl_3$): δ 8.23 (d, 2H, CH), 7.85 (t, 1H, CH), 7.47 (t, 2H, CH), 7.35 (s, 2H, CH), 7.27 (s, 2H, CH), 7.25 (s, 2H, CH), 4.01 (m, 2H, CH_2), 3.28 (m, 2H, CH_2), 2.57 (s, 6H, CH_3), 2.55 (s, 6H, CH_3), 2.38 (s, 6H, CH_3), 2.32 (t, 4H, CH_2), 2.31 (t, 4H, CH_2), 2.00 (m, 4H, CH_2), 1.81 (s, 6H, CH_3), 1.77 (s, 6H, CH_3), 1.70 (m, 4H, CH_2), 1.30 (s, 6H, CH_3), 1.05 (t, 6H, CH_3), 1.00 (t, 6H, CH_3). ^{13}C NMR (126 MHz, $CDCl_3$): δ 174.55, 155.40, 154.20, 150.74, 139.14, 138.61, 138.55, 138.27, 138.00, 137.59, 137.21, 136.40, 133.93, 133.13, 131.08, 130.05, 129.68, 129.39, 126.71, 126.66, 83.22, 64.92, 32.65, 29.50, 18.50, 18.30, 17.28, 17.22, 14.79, 14.62, 13.06, 12.73, 12.06. ^{19}F NMR ($CDCl_3$, 471 MHz): δ −81.21 (s, 3F, CF_3), −148.84 (m, 4F, BF_2). ESI HR-MS *m*/*z*: calcd for $C_{61}H_{74}IrB_2F_4N_6$ $[M - H]^+$, 1410.57415; found, 1410.57436.

Synthesis of [IrCl(CO)$_2$(4)]. To a Schlenk flask (10 mL) equipped with stirring bar and septum were added [IrCl(cod)(**4**)] (40 mg, 0.0329 mmol) and dry CH_2Cl_2 (5 mL). A balloon with carbon monoxide was connected through a cannula, and CO was bubbled through the stirred solution during 30 min. The reaction mixture was concentrated under reduced pressure, then pentane was added, and the resulting precipitate was filtered off and washed with pentane. The resulting product is an orange solid (30 mg, 0.0258 mmol, yield 78%).

^{1}H NMR (300 MHz, $CDCl_3$): δ 7.35 (s, 2H, N−*CH*−*CH*−N), 7.19 (s, 4H, 4H *m*-Ar), 2.55 (s, 12H), 2.33−2.30 (m, 20H, 4× CH_3, 4× CH_2 Bodipy), 1.49 (s, 12H), 1.05−0.98 (m, 12H, 4× CH_3 Bodipy). ^{13}C NMR (126 MHz, $CDCl_3$): δ 179.75, 176.87, 168.48, 155.07, 153.34, 139.54, 138.81, 137.67, 137.32, 136.88, 133.53, 132.70, 131.11, 128.71, 123.82, 18.82, 17.24, 14.83, 14.70, 12.95, 12.78, 12.64, 12.36. ^{19}F NMR (471 MHz, $CDCl_3$): δ −148.77, −148.98 (m, 4F, BF_2). ESI HR-MS *m*/*z*: calcd for $C_{55}H_{63}IrB_2ClF_4N_6O_2$ $[M - H]^+$, 1165.44470; found, 1165.44588.

Synthesis of [PdCl(allyl)(4)]. **4**·HCl (50 mg, 0.0545 mmol, 1 equiv), $[PdCl(allyl)]_2$ (10.0 mg, 0.0273 mol, 0.5 equiv), and K_2CO_3 (22.6 mg, 0.164 mmol, 3 equiv) were suspended in acetone (3 mL). Next, the mixture was stirred at 60 °C for 4 h. The volatiles were removed in vacuo, and CH_2Cl_2 (3 mL) was added to the residue. The mixture was filtered through a silica plug and the filtrate dried in vacuo. The solution was evaporated and purified by column chromatography (Cy/EA 1:1). An orange solid was obtained (40 mg, 0.0376 mmol, 69%).

^{1}H NMR (500 MHz, $CDCl_3$): δ 7.28 (s, 2H, N−*CH*−*CH*−N), 7.19−7.09 (m, 4H, 4H *m*-Ar), 4.85 (m, 1H, allyl), 3.94−3.87 (m, 1H, allyl), 3.32 (d, J = 6.5 Hz, 1H, allyl), 2.79 (d, J = 13.5 Hz, 1H, allyl), 2.53 (m, 12H, 4× CH_3), 2.34−2.27 (m, 20H, 4× CH_3, 4× CH_2 Bodipy), 1.97 (d, J = 12.0 Hz, 1H, allyl), 1.45 (s, 6H, 2× CH_3), 1.37 (s, 6H, 2× CH_3), 1.08−0.92 (m, 12H, 4× CH_3 Bodipy). ^{13}C NMR (126 MHz, $CDCl_3$): δ 184.82, 154.69, 153.60, 139.04, 138.73, 138.66, 137.60, 137.25, 137.08, 133.32, 132.80, 130.87, 130.37, 128.47, 123.38, 114.19, 72.85, 49.30, 29.81, 18.52, 18.49, 17.24, 17.16, 14.77, 14.71, 12.70, 12.61, 12.56, 12.18, 1.13. ^{19}F NMR (282 MHz, $CDCl_3$): δ −148.79, −149.13 (m, 4F, BF_2). ESI HR-MS *m*/*z*: calcd for $C_{56}H_{67}B_2F_4N_6Pd$ $[M]^+$, 1027.457882; found, 1027.460295.

Synthesis of [PdCl$_2$(Clpy)(4)]. A Schlenk flask equipped with a stirring bar was loaded with imidazolium salt **4**·HCl (50 mg, 0.0545 mmol, 1 equiv), $PdCl_2$ (9.67 mg, 0.0545 mmol, 1 equiv), and K_2CO_3 (37.7 mg, 0.273 mmol, 5 equiv). 3-Chloropyridine (1.0 mL) was added, and the mixture was stirred at 80 °C in a sealed flask overnight. The reaction mixture was filtered through Celite, and the filtrate was evaporated under reduced pressure. The orange residue was dissolved in a minimum amount of CH_2Cl_2, filtered, and precipitated with *n*-pentane. The product was obtained as an orange solid (54 mg, 0.0461 mmol, 85%).

^{1}H NMR (500 MHz, CD_2Cl_2): δ 8.62 (d, J = 2.4 Hz, 1H), 8.52 (dd, J = 5.6, 1.4 Hz, 1H), 7.75 (dt, J = 8.4, 1.7 Hz, 1H), 7.32 (s, 2H), 7.26 (s, 5H), 7.24−7.18 (m, 1H), 2.59−2.50 (m, 16H), 2.47 (s, 14H), 2.39 (q, J = 7.6 Hz, 4H), 2.31 (q, J = 7.6 Hz, 4H), 1.62 (s, 7H), 1.56 (s, 7H), 1.05 (t, J = 7.5 Hz, 6H), 0.99 (t, J = 7.5 Hz, 7H). ^{13}C NMR (126 MHz, CD_2Cl_2): δ 154.68, 154.11, 153.35, 150.69, 149.79, 140.16, 139.64, 138.73, 138.61, 138.56, 137.48, 133.74, 133.50, 132.56, 131.37, 130.86, 128.98, 125.14, 124.98, 30.29, 19.67, 17.64, 17.61, 15.05, 15.00, 13.29, 12.89, 12.62. ^{19}F NMR (471 MHz, CD_2Cl_2): δ −147.78, −147.99 (m, 4F, BF_2). ESI HR-MS *m*/*z*: calcd for $C_{58}H_{67}B_2Cl_3F_4N_7Pd$ $[M]^+$, 1170.36751; found, 1170.37199.

Synthesis of [AuCl(4)]. To a round-bottom flask (5 mL) equipped with a stirring bar were added imidazolium salt **4**·HCl (50 mg, 0.0545 mmol, 1 equiv), $[AuCl(Me_2S)]$ (16.1 mg, 0.0545 mmol, 1 equiv), K_2CO_3 (7.5 mg, 0.0545 mmol, 1 equiv), and acetone (3 mL). The flask was sealed, and the reaction mixture was stirred at 60 °C for 12 h. The solution was filtered, evaporated, and purified by column chromatography (Cy/EA). The volatiles were removed to

DOI: 10.1021/acs.organomet.9b00130
Organometallics XXXX, XXX, XXX−XXX

provide complex [AuCl(**3**)] as a yellow solid (16 mg, 0.0144 mmol, yield 26%).

^{1}H NMR (500 MHz, $CDCl_3$): δ 7.35 (s, 2H, N−*CH*−*CH*−N), 7.22 (s, 4H, 4H *m*-Ar), 2.54 (d, J = 3.8 Hz, 12H), 2.37−2.29 (m, 8H, 4× CH_2 Bodipy), 2.24 (s, 12H), 1.49 (s, 6H), 1.42 (s, 6H), 1.05−0.96 (m, 12H, 4× CH_3 Bodipy). ^{13}C NMR (126 MHz, $CDCl_3$): δ 175.12, 155.50, 153.25, 139.99, 138.35, 138.25, 137.65, 137.03, 136.48, 133.97, 132.64, 131.17, 129.99, 129.06, 122.32, 18.06, 17.27, 17.19, 14.83, 14.66, 12.92, 12.77, 12.62, 12.39. ^{19}F NMR (471 MHz, $CDCl_3$): δ −148.79, −149.00 (m, m, 4F, BF_2). ESI HR-MS m/z: calcd for $C_{53}H_{63}AuB_2ClF_4N_6$ $[M - H]^+$, 1113.45852; found, 1113.45894.

Synthesis of [NiCl(Cp)(4)]. A Schlenk flask equipped with a stirring bar was loaded with imidazolium salt **4**·HCl (50 mg, 0.0545 mmol, 1 equiv) and nickelocene (10.2 mg, 0.0545 mmol, 1 equiv). Next, THF (10 mL) was added and the reaction mixture was heated to reflux for 24 h. The solvent was removed under vacuum, and the resulting red residue was purified by column chromatography. Evaporation of the solvent under reduced pressure provides the desired product as a dark reddish solid (35 mg, 0.0337 mmol, yield 62%).

^{1}H NMR (500 MHz, CD_2Cl_2): δ 7.34 (s, 4H, 4H *m*-Ar), 7.25 (s, 2H, N−*CH*−*CH*−N), 4.70 (s, 5H, CH, Cp), 2.54 (s, 12H), 2.46−2.34 (m, 8H, 4× CH_2 Bodipy), 2.26 (s, 12H), 1.85 (s, 6H), 1.49 (s, 6H), 1.05 (t, J = 7.6 Hz, 12H, 4× CH_3 Bodipy). ^{13}C NMR (126 MHz, CD_2Cl_2): δ 167.99, 155.00, 154.04, 140.29, 140.06, 139.70, 138.62, 138.40, 137.51, 133.92, 133.53, 131.27, 131.06, 129.20, 125.61, 92.70, 18.88, 17.63, 15.03, 15.00, 13.38, 12.95, 12.86, 12.37. ^{19}F NMR (282 MHz, CD_2Cl_2): δ −147.72, −148.07 (m, 4F, BF_2). ESI HR-MS m/z: calcd for $C_{58}H_{67}B_2F_4Ni$ $[M - Cl]^+$, 1003.48974; found, 1003.49013.

Synthesis of [$PdCl_2$(3)]. In an oven-dried Schlenk flask, diimine **3** (50 mg, 0.0576 mmol, 1 equiv) and $[PdCl_2(CH_3CN)_2]$ (14.9 mg, 0.0576 mmol, 1 equiv) were dissolved in CH_2Cl_2 (10 mL). An orange solid immediately precipitated from the solution, and the reaction mixture was left to stir for 12 h. The resulting suspension was filtered off and washed with diethyl ether. The resulting solid was dried under reduced pressure to give an orange solid (43 mg, 0.0411 mmol, 71%). The [$PdCl_2$(**3**)] is poorly soluble in $CDCl_3$. ^{1}H NMR (300 MHz, $CDCl_3$): δ 8.35 (s, 2H, N=*CH*−*CH*=N), 7.12 (s, 4H, 4× H *m*-Ar), 2.53 (s, 12H, 2× CH_3 Bodipy), 2.43 (s, 12H, 2× CH_3 Bodipy), 2.29 (q, J = 6.9, 6.4 Hz, 8H, 4× CH_2 Bodipy), 1.44 (s, 6H, CH_3 Bodipy), 1.37 (s, 6H, CH_3 Bodipy), 0.97 (t, J = 6.9 Hz, 12H, 2× CH_3 Bodipy). ^{13}C NMR insufficient solubility. ESI HR-MS m/z: calcd for $C_{54}H_{65}B_2ClF_4N_7Pd$ $[M-Cl + CH_3CN]^+$, 1050.41416; found, 1050.41716.

Synthesis of [PdCl(CH_3)(3)]. To a solution of diimine **3** (50 mg, 0.0576 mmol, 1 equiv) in dry CH_2Cl_2 (10 mL) was added [Pd(cod)MeCl] (16.0 mg, 0.0604 mmol, 1.05 equiv). After stirring the mixture for 12 h at room temperature, the volatiles were evaporated to give an orange residue. The residue was dissolved in a minimum amount of dichloromethane and added to diethyl ether. Pentane was added to precipitate the product. The remaining solid was dried in vacuo to provide the product as an orange solid (36 mg, 0.0351 mmol, 61%).

^{1}H NMR (500 MHz, CD_2Cl_2): δ 8.48 (s, 1H, N=CH−*CH*=N), 8.34 (s, 1H, N=*CH*−CH=N), 7.18 (s, 2H, 2× H *m*-Ar), 7.11 (s, 2H, 2× H *m*-Ar), 2.51 (s, 6H, CH_3 Bodipy), 2.50 (s, 6H, CH_3 Bodipy), 2.39 (s, 6H, 2× CH_3 Bodipy), 2.37−2.31 (m, 14H, CH_3 Bodipy, 2× CH_2 Bodipy), 1.48 (d, J = 12.1 Hz, 6H, 2× CH_3 Bodipy), 1.45 (s, 6H, 2× CH_3 Bodipy), 1.03−0.99 (m, 12H, 4× CH_3 Bodipy), 0.69 (s, 3H, CH_3−Pd). ^{13}C NMR (126 MHz, CD_2Cl_2): δ 165.52, 161.04, 155.01, 154.13, 153.44, 147.32, 146.79, 140.76, 140.35, 139.62, 139.55, 138.44, 138.34, 135.68, 134.88, 133.95, 133.47, 133.13, 131.67, 131.35, 130.75, 129.98, 129.07, 128.56, 18.97, 18.42, 17.60, 15.05, 15.01, 14.95, 12.91, 12.51, 12.47, 3.01. ESI HR-MS m/z: calcd for $C_{55}H_{68}B_2F_4N_7Pd$ $[M-Cl + CH_3CN]^+$, 1030.46878; found, 1030.47204.

Synthesis of Polyethylene. Under an inert atmosphere, a 25 mL Schlenk flask was charged with NaBArF (1.2 equiv), 15 mL of 1,2-dichloroethane, and a stirring bar, and the solution was saturated with ethylene during ca. 60 min. A stock solution of precatalyst [$PdCl(CH_3)$(**3**)] (c = 2.5 × 10^{-5} M, 1 mL) in 1,2-dichloroethane was injected with stirring to initiate polymerization. After 24 h, the polymerization was quenched via the addition of MeOH (5 mL), leading to the precipitation of the polymer. ^{1}H NMR (500 MHz, $CDCl_3$): δ 1.36−1.17 (m, CH_2), 0.89−0.82 (m, CH_3). ^{13}C NMR (126 MHz, $CDCl_3$): δ 32.10, 30.21, 29.87, 29.52, 27.29, 26.92, 22.85, 14.27.

Synthesis of [Mo(CO_4)(3)]. A Schlenk flask equipped with a stirring bar was loaded with diimine **3** (32.9 mg, 0.0379 mmol, 1 equiv) and $Mo(CO)_6$ (10.0 mg, 0.0379 mmol, 1 equiv). THF (6 mL) was added and heated to reflux for 18 h. The solvent was removed under vacuum, and the remaining red residue was purified by flash column chromatography (Cy/EA 8:1). Evaporation of the solvent under reduced pressure provides the desired product as a dark violet solid (18 mg, 0.0167 mmol, yield 44%).

^{1}H NMR (500 MHz, C_6D_6): δ 7.26 (s, 2H), 6.63 (s, 4H), 2.73 (s, 6H), 2.67 (s, 6H), 2.18 (q, J = 7.5 Hz, 4H), 2.11−2.06 (m, 16H), 1.65 (s, 6H), 1.51 (s, 6H), 0.92 (t, J = 7.6 Hz, 6H), 0.84 (t, J = 7.6 Hz, 6H). ^{13}C NMR (126 MHz, C_6D_6): δ 158.91, 155.62, 153.53, 152.94, 139.87, 139.45, 136.82, 134.74, 133.79, 132.59, 131.91, 131.05, 129.45, 129.10, 17.97, 17.45, 17.31, 14.98, 14.75, 12.98, 12.89, 12.66, 12.27 (CO resonances could not be observed. This has been reported before in the literature for similar complexes).[65] ESI HR-MS m/z: calcd for $C_{56}H_{63}B_2F_4MoN_6O_4$ $[M + H]^+$, 1079.408163; found, 1051.409190. IR ν(CO): 2015, 1916, 1885 cm^{-1}.

■ ASSOCIATED CONTENT

Supporting Information

The Supporting Information is available free of charge on the ACS Publications website at DOI: 10.1021/acs.organomet.9b00130.

Full experiment, NMR spectra, fluorescence measurements, fluorescence spectra, cyclic voltammetry, and mass spectrometry (PDF)

■ AUTHOR INFORMATION

Corresponding Author

*E-mail: plenio@tu-darmstadt.de.

ORCID

Oliver Halter: 0000-0002-6680-0276

Yuki Kanai: 0000-0001-9561-861X

Herbert Plenio: 0000-0002-2257-983X

Notes

The authors declare no competing financial interest.

■ ACKNOWLEDGMENTS

This work was supported by the DFG via grant Pl178/18-1 and Pl178/18-2. Generous support with gold salts by Heraeus is acknowledged. We wish to thank B. Sc. Markus Frank for the synthesis of two [(*N*,*N*-diaryl-diimine)$Mo(CO)_4$] complexes.

■ REFERENCES

(1) (a) Callan, J. F.; de Silva, A. P.; Magri, D. C. Luminescent sensors and switches in the early 21st century. *Tetrahedron* **2005**, *61*, 8551−8588. (b) Bertrand, B.; Passador, K.; Goze, C.; Denat, F.; Bodio, E.; Salmain, M. Metal-based BODIPY derivatives as multimodal tools for life sciences. *Coord. Chem. Rev.* **2018**, *358*, 108−124. (c) Cordes, T.; Blum, S. A. Opportunities and challenges in single-molecule and single-particle fluorescence microscopy for mechanistic studies of chemical reactions. *Nat. Chem.* **2013**, *5*, 993−999.

(2) (a) Daly, B.; Ling, J.; de Silva, A. P. Current developments in fluorescent PET (photoinduced electron transfer) sensors and switches. *Chem. Soc. Rev.* **2015**, *44*, 4203−4211. (b) Urano, Y.; Kamiya, M.; Kanda, K.; Ueno, T.; Hirose, K.; Nagano, T. Evolution of

DOI: 10.1021/acs.organomet.9b00130
Organometallics XXXX, XXX, XXX−XXX

Fluorescein as a Platform for Finely Tunable Fluorescence Probes. *J. Am. Chem. Soc.* **2005**, *127*, 4888−4894. (c) Ueno, T.; Urano, Y.; Setsukinai, K.-i.; Takakusa, H.; Kojima, H.; Kikuchi, K.; Ohkubo, K.; Fukuzumi, S.; Nagano, T. Rational Principles for Modulating Fluorescence Properties of Fluorescein. *J. Am. Chem. Soc.* **2004**, *126*, 14079−14085. (d) Gabe, Y.; Urano, Y.; Kikuchi, K.; Kojima, H.; Nagano, T. Highly Sensitive Fluorescence Probes for Nitric Oxide Based on Boron Dipyrromethene Chromophore Rational Design of Potentially Useful Bioimaging Fluorescence Probe. *J. Am. Chem. Soc.* **2004**, *126*, 3357−3367.

(3) Lakowicz, J. R. *Principles of Fluorescence Spectroscopy*; Springer-Verlag: New York, 2010.

(4) Hartwig, J. F. *Organotransition Metal Chemistry: From Bonding to Catalysis*; University Science Books: Sausalito, 2010.

(5) Halter, O.; Vasiuta, R.; Fernández, I.; Plenio, H. Systematic Modulation of the Fluorescence Brightness in Boron-Dipyrromethene (BODIPY)-Tagged N-Heterocyclic Carbene (NHC)-Gold-Thiolates. *Chem.—Eur. J.* **2016**, *22*, 18066−18072.

(6) (a) Kiel, A.; Kovacs, J.; Mokhir, A.; Krämer, R.; Herten, D.-P. Direct Monitoring of Formation and Dissociation of Individual Metal Complexes by Single-Molecule Fluorescence Spectroscopy. *Angew. Chem., Int. Ed.* **2007**, *46*, 3363−3366. (b) Brox, D.; Kiel, A.; Wörner, S. J.; Pernpointner, M.; Comba, P.; Martin, B.; Herten, D.-P. Ensemble and Single-Molecule Studies on Fluorescence Quenching in Transition Metal Bipyridine-Complexes. *PLoS One* **2013**, *8*, No. e58049. (c) Rybina, A.; Lang, C.; Wirtz, M.; Grußmayer, K.; Kurz, A.; Maier, F.; Schmitt, A.; Trapp, O.; Jung, G.; Herten, D.-P. Distinguishing Alternative Reaction Pathways by Single-Molecule Fluorescence Spectroscopy. *Angew. Chem., Int. Ed.* **2013**, *52*, 6322−6325.

(7) Feng, C.; Cunningham, D. W.; Easter, Q. T.; Blum, S. A. Role of LiCl in Generating Soluble Organozinc Reagents. *J. Am. Chem. Soc.* **2016**, *138*, 11156−11159.

(8) (a) Easter, Q. T.; Blum, S. A. Single Turnover at Molecular Polymerization Catalysts Reveals Spatiotemporally Resolved Reactions. *Angew. Chem., Int. Ed.* **2017**, *56*, 13772−13775. (b) Easter, Q. T.; Blum, S. A. Evidence for Dynamic Chemical Kinetics at Individual Molecular Ruthenium Catalysts. *Angew. Chem., Int. Ed.* **2018**, *57*, 1572−1575. (c) Easter, Q. T.; Trauschke, V.; Blum, S. A. Catalyst Inefficiencies: Supported Ring-Opening Metathesis Polymerization Catalyst Yields Its Ensemble Rate from a Small Number of Molecular Active Sites. *ACS Catal.* **2015**, *5*, 2290−2295. (d) Esfandiari, N. M.; Blum, S. A. Homogeneous vs Heterogeneous Polymerization Catalysis Revealed by Single-Particle Fluorescence Microscopy. *J. Am. Chem. Soc.* **2011**, *133*, 18145−18147.

(9) Ng, J. D.; Upadhyay, S. P.; Marquard, A. N.; Lupo, K. M.; Hinton, D. A.; Padilla, N. A.; Bates, D. M.; Goldsmith, R. H. Single-Molecule Investigation of Initiation Dynamics of an Organometallic Catalyst. *J. Am. Chem. Soc.* **2016**, *138*, 3876−3883.

(10) Scheinhardt, B.; Trzaskowski, J.; Baier, M. C.; Stempfle, B.; Oppermann, A.; Wöll, D.; Mecking, S. Anisotropic Polyethylene Nanocrystals Labeled with a Single Fluorescent Dye Molecule: Toward Monitoring of Nanoparticle Orientation. *Macromolecules* **2013**, *46*, 7902−7910.

(11) Sashuk, V.; Schoeps, D.; Plenio, H. Fluorophore tagged Cross-Coupling Catalysts. *Chem. Commun.* **2009**, 770−772.

(12) Loudet, A.; Burgess, K. BODIPY Dyes and Their Derivatives: Syntheses and Spectroscopic Properties. *Chem. Rev.* **2007**, *107*, 4891−4932.

(13) (a) Ulrich, G.; Ziessel, R.; Harriman, A. The Chemistry of Fluorescent Bodipy Dyes: Versatility Unsurpassed. *Angew. Chem., Int. Ed.* **2008**, *47*, 1184−1201. (b) Boens, N.; Leen, V.; Dehaen, W. Fluorescent indicators based on BODIPY. *Chem. Soc. Rev.* **2012**, *41*, 1130−1172. (c) Boens, N.; Verbelen, B.; Dehaen, W. Postfunctionalization of the BODIPY Core: Synthesis and Spectroscopy. *Eur. J. Org. Chem.* **2015**, *2015*, 6577−6595. (d) Wu, D.; Sedgwick, A. C.; Gunnlaugsson, T.; Akkaya, E. U.; Yoon, J.; James, T. D. Fluorescent chemosensors: the past, present and future. *Chem. Soc. Rev.* **2017**, *46*, 7105−7123.

(14) (a) Kos, P.; Plenio, H. Metal Complexes of a Boron-Dipyrromethene (BODIPY)-Tagged N-Heterocyclic Carbene (NHC) as Luminescent Carbon Monoxide Chemodosimeters. *Chem.—Eur. J.* **2015**, *21*, 1088−1095. (b) Lifschitz, A. M.; Shade, C. M.; Spokoyny, A. M.; Mendez-Arroyo, J.; Stern, C. L.; Sarjeant, A. A.; Mirkin, C. A. Boron-Dipyrromethene-Functionalized Hemilabile Ligands as "Turn-On" Fluorescent Probes for Coordination Changes in Weak-Link Approach Complexes. *Inorg. Chem.* **2013**, *52*, 5484−5492.

(15) (a) Sashuk, V.; Peeck, L. H.; Plenio, H. [$RuCl_2$(CHPh)-(NHC)(NHC_{ewg})] Complexes with Modified NHC_{ewg} Ligands for Efficient Ring-Closing Metathesis Leading to Tetrasubstituted Olefins. *Chem.—Eur. J.* **2010**, *16*, 3983−3993. (b) Hensle, E. M.; Esfandiari, N. M.; Lim, S.-G.; Blum, S. A. BODIPY Fluorophore Toolkit for Probing Chemical Reactivity and for Tagging Reactive Functional Groups. *Eur. J. Org. Chem.* **2014**, *2014*, 3347−3354. (c) Irmler, P.; Winter, R. F. Complexes trans-Pt(BODIPY)X(PEt_3)$_2$: excitation energy-dependent fluorescence and phosphorescence emissions, oxygen sensing and photocatalysis. *Dalton Trans.* **2016**, *45*, 10420−10434. (d) Geist, F.; Jackel, A.; Winter, R. F. Ligand Based Dual Fluorescence and Phosphorescence Emission from BODIPY Platinum Complexes and Its Application to Ratiometric Singlet Oxygen Detection. *Inorg. Chem.* **2015**, *54*, 10946−10957.

(16) Vorfalt, T.; Wannowius, K. J.; Thiel, V.; Plenio, H. How Important Is the Release-Return Mechanism in Olefin Metathesis? *Chem.—Eur. J.* **2010**, *16*, 12312−12315.

(17) Vasiuta, R.; Plenio, H. Observing Initial Steps in Gold-Catalyzed Alkyne Transformations by Utilizing Bodipy-Tagged Phosphine-Gold Complexes. *Chem.—Eur. J.* **2016**, *22*, 6353−6360.

(18) Halter, O.; Fernández, I.; Plenio, H. Fine-Tuning the Fluorescence Gain of FRET-Type (Bodipy)(Bodipy′)-NHC-Iridium Complexes for CO Detection with a Large Virtual Stokes Shift. *Chem.—Eur. J.* **2017**, *23*, 711−719.

(19) Kos, P.; Plenio, H. A Fluorescent Molecular Probe for the Detection of Hydrogen Based on Oxidative Addition Reactions with Crabtree-Type Hydrogenation Catalysts. *Angew. Chem., Int. Ed.* **2015**, *54*, 13293−13296.

(20) Halter, O.; Plenio, H. Fluorescence resonance energy transfer (FRET) for the verification of dual gold catalysis. *Chem. Commun.* **2017**, *53*, 12461−12464.

(21) (a) Kim, K. H.; Ok, T.; Lee, K.; Lee, H.-S.; Chang, K. T.; Ihee, H.; Sohn, J.-H. Quantitative Catalyst−Substrate Association Relationships between Metathesis Molybdenum or Ruthenium Carbene Complexes and Their Substrates. *J. Am. Chem. Soc.* **2010**, *132*, 12027−12033. (b) Lee, J.; Kim, K. H.; Lee, O. S.; Choi, T.-L.; Lee, H.-S.; Ihee, H.; Sohn, J.-H. Preference of Ruthenium-Based Metathesis Catalysts toward Z- and E-Alkenes as a Guide for Selective Reactions to Alkene Stereoisomers. *J. Org. Chem.* **2016**, *81*, 7591−7596. (c) Sohn, J.-H.; Kim, K. H.; Lee, H.-Y.; No, Z. S.; Ihee, H. Initial Catalyst−Substrate Association Step in Enyne Metathesis Catalyzed by Grubbs Ruthenium Complex Probed by Time-Dependent Fluorescence Quenching. *J. Am. Chem. Soc.* **2008**, *130*, 16506−16507.

(22) Irmler, P.; Winter, R. F. σ-Pt-BODIPY Complexes with Platinum Attachment to Carbon Atoms C2 or C3: Spectroscopic, Structural, and (Spectro)Electrochemical Studies and Photocatalysis. *Organometallics* **2018**, *37*, 235−253.

(23) Halter, O.; Plenio, H. Fluorescent Dyes in Organometallic Chemistry: Coumarin-Tagged NHC-Metal Complexes. *Eur. J. Inorg. Chem.* **2018**, 2935−2943.

(24) Ittel, S. D.; Johnson, L. K.; Brookhart, M. Late-Metal Catalysts for Ethylene Homo- and Copolymerization. *Chem. Rev.* **2000**, *100*, 1169−1204.

(25) Liedholm, B. Simple synthetic route to 4-aminobenzaldehydes from anilines. *J. Chem. Soc., Perkin Trans. 1* **1992**, 2235−2237.

(26) Grimblat, N.; Sarotti, A. M.; Kaufman, T. S.; Simonetti, S. O. A theoretical study of the Duff reaction: insights into its selectivity. *Org. Biomol. Chem.* **2016**, *14*, 10496−10501.

DOI: 10.1021/acs.organomet.9b00130
Organometallics XXXX, XXX, XXX−XXX

(27) Pochorovski, I.; Breiten, B.; Schweizer, W. B.; Diederich, F. FRET Studies on a Series of BODIPY-Dye-Labeled Switchable Resorcin[4]arene Cavitands. *Chem.—Eur. J.* **2010**, *16*, 12590−12602.
(28) Leuthäußer, S.; Schwarz, D.; Plenio, H. Tuning the electronic properties of N-heterocyclic Carbenes. *Chem.—Eur. J.* **2007**, *13*, 7195−7203.
(29) Fleckenstein, C.; Roy, S.; Leuthäußer, S.; Plenio, H. Sulfonated N-heterocyclic carbenes for Suzuki coupling in water. *Chem. Commun.* **2007**, 2870−2872.
(30) Hintermann, L. Expedient syntheses of the N-heterocyclic carbene precursor imidazolium salts IPr·HCl, IMes·HCl and IXy·HCl. *Beilstein J. Org. Chem.* **2007**, *3*, 22−26.
(31) Nelson, D. J. Accessible Syntheses of Late Transition Metal (Pre)Catalysts Bearing N-Heterocyclic Carbene Ligands. *Eur. J. Inorg. Chem.* **2015**, 2012−2027.
(32) Ramon, R. S.; Nolan, S. P. N-Heterocyclic Carbenes. In *Applied Homogeneous Catalysis with Organometallic Compounds*; Cornils, B., Herrmann, w. A., Beller, M., Paciello, R., Eds.; Wiley-VCH, 2017.
(33) Dai, S.; Sui, X.; Chen, C. Highly Robust Palladium(II) α-Diimine Catalysts for Slow-Chain-Walking Polymerization of Ethylene and Copolymerization with Methyl Acrylate. *Angew. Chem., Int. Ed.* **2015**, *54*, 9948−9953.
(34) (a) Guo, L.; Dai, S.; Sui, X.; Chen, C. Palladium and Nickel Catalyzed Chain Walking Olefin Polymerization and Copolymerization. *ACS Catal.* **2016**, *6*, 428−441. (b) Kanai, Y.; Foro, S.; Plenio, H. Bispentiptycenyl-Diimine-Nickel Complexes for Ethene Polymerization and Copolymerization with Polar Monomers. *Organometallics* **2019**, *38*, 544−551.
(35) (a) Fedushkin, I. L.; Skatova, A. A.; Lukoyanov, A. N.; Khvoinova, N. M.; Piskunov, A. V.; Nikipelov, A. S.; Fukin, G. K.; Lysenko, K. A.; Irran, E.; Schumann, H. 1,2-Bis(imino)acenaphthene complexes of molybdenum and nickel. *Dalton Trans.* **2009**, 4689−4694. (b) Dieck, H. t.; Renk, I. W. Zur Komplexchemie von Vierzentren-π-Systemen, III. Farbe, Solvatochromie und Reduktionspotentiale der 1.4-Diaza-butadien-molybdäntetracarbonyle. *Chem. Ber.* **1971**, *104*, 110−130.
(36) Savka, R.; Plenio, H. Facile synthesis of [(NHC)MX(cod)] and [(NHC)MCl(CO)$_2$] (M = Rh, Ir; X = Cl, I) complexes. *Dalton Trans.* **2015**, *44*, 891−893.
(37) Bergmann, M.; Savka, R.; Foro, S.; Plenio, H. Synthesis of an ortho -Methyl-N ,N′ -bis(triptycenyl) N-Heterocyclic Carbene Ligand and Its Metal Complexes. *Eur. J. Inorg. Chem.* **2017**, 3779−3786.
(38) (a) Visbal, R.; Laguna, A.; Gimeno, M. C. Simple and efficient synthesis of [MCI(NHC)] (M = Au, Ag) complexes. *Chem. Commun.* **2013**, *49*, 5642−5644. (b) Collado, A.; Gómez-Suárez, A.; Martin, A. R.; Slawin, A. M. Z.; Nolan, S. P. Straightforward synthesis of [Au(NHC)X] (NHC = N-heterocyclic carbene, X = Cl, Br, I) complexes. *Chem. Commun.* **2013**, *49*, 5541−5543.
(39) Kelly, R. A.; Scott, N. M.; Díez-González, S.; Stevens, E. D.; Nolan, S. P. Simple Synthesis of CpNi(NHC)Cl Complexes (Cp = Cyclopentadienyl; NHC = N-Heterocyclic Carbene). *Organometallics* **2005**, *24*, 3442−3447.
(40) (a) Wolf, S.; Plenio, H. Synthesis of (NHC)Rh(cod)Cl and (NHC)Rh(CO)$_2$Cl Complexes − Translation of the Rh- into the Ir-Scale for the electronic Properties of NHC Ligands. *J. Organomet. Chem.* **2009**, *694*, 1487−1492. (b) Huynh, H. V. Electronic Properties of N-Heterocyclic Carbenes and Their Experimental Determination. *Chem. Rev.* **2018**, *118*, 9457−9492.
(41) Hansch, C.; Leo, A.; Taft, R. W. A Survey of Hammett Substituent Constants and Resonance and Field Parameters. *Chem. Rev.* **1991**, *91*, 165−195.
(42) Nepomnyashchii, A. B.; Bard, A. J. Electrochemistry and Electrogenerated Chemiluminescence of BODIPY Dyes. *Acc. Chem. Res.* **2012**, *45*, 1844−1853.
(43) (a) Leuthäußer, S.; Schmidts, V.; Thiele, C. M.; Plenio, H. π-Face Donor Properties of N-Heterocyclic Carbenes in Grubbs II Complexes. *Chem.—Eur. J.* **2008**, *14*, 5465−5481. (b) Credendino, R.; Falivene, L.; Cavallo, L. π-Face Donation from the Aromatic N-Substituent of N-Heterocyclic Carbene Ligands to Metal and Its Role in Catalysis. *J. Am. Chem. Soc.* **2012**, *134*, 8127−8135.
(44) Ardizzoia, G. A.; Bea, M.; Brenna, S.; Therrien, B. A Quantitative Description of the σ-Donor and π-Acceptor Properties of Substituted Phenanthrolines. *Eur. J. Inorg. Chem.* **2016**, 3829−3837.
(45) Würth, C.; Grabolle, M.; Pauli, J.; Spieles, M.; Resch-Genger, U. Relative and absolute determination of fluorescence quantum yields of transparent samples. *Nat. Protoc.* **2013**, *8*, 1535−1550.
(46) Fleckenstein, C. A.; Plenio, H. Sterically demanding Trialkylphosphines for Palladium-catalyzed Cross Coupling Reactions—Alternatives to P*t*Bu$_3$. *Chem. Soc. Rev.* **2010**, *39*, 694−711.
(47) Navarro, M.; Wang, S.; Müller-Bunz, H.; Redmond, G.; Farràs, P.; Albrecht, M. Triazolylidene Metal Complexes Tagged with a Bodipy Chromophore: Synthesis and Monitoring of Ligand Exchange Reactions. *Organometallics* **2017**, *36*, 1469−1478.
(48) Ahrens, J.; Haberlag, B.; Scheja, A.; Tamm, M.; Bröring, M. Conjugated BODIPY DYEmers by Metathesis Reactions. *Chem.—Eur. J.* **2014**, *20*, 2901−2912.
(49) Redón, R.; Torrens, H.; Wang, Z.; Morales-Morales, D. Allyl−palladium complexes with fluorinated benzene thiolate ligands. Examination of the electronic effects in the Pd-catalyzed allylic alkylation reaction with the catalytic system [(η^3-C$_3$H$_5$)Pd(μ-SR$_f$)]$_2$/PR$_3$. *J. Organomet. Chem.* **2002**, *654*, 16−20.
(50) The fluorescence level of this complex is arbitrarily set to 1.0 in all fluorescence experiments.
(51) (a) Yakelis, N. A.; Bergman, R. G. Safe Preparation and Purification of Sodium Tetrakis[(3,5-trifluoromethyl)phenyl]borate (NaBArF$_{24}$): Reliable and Sensitive Analysis of Water in Solutions of Fluorinated Tetraarylborates. *Organometallics* **2005**, *24*, 3579−3581. (b) Gatto, M.; Belanzoni, P.; Belpassi, L.; Biasiolo, L.; Del Zotto, A.; Tarantelli, F.; Zuccaccia, D. Solvent-, Silver-, and Acid-Free NHC-Au-X Catalyzed Hydration of Alkynes. The Pivotal Role of the Counterion. *ACS Catal.* **2016**, *6*, 7363−7376.
(52) Popeney, C.; Guan, Z. Ligand Electronic Effects on Late Transition Metal Polymerization Catalysts. *Organometallics* **2005**, *24*, 1145−1155.
(53) Brown, T. J.; Widenhoefer, R. A. Cationic Gold(I) π-Complexes of Terminal Alkynes and Their Conversion to Dinuclear σ,π-Acetylide Complexes. *Organometallics* **2011**, *30*, 6003−6009.
(54) Mecking, S.; Johnson, L. K.; Wang, L.; Brookhart, M. Mechanistic Studies of the Palladium-Catalyzed Copolymerization of Ethylene and α-Olefins with Methyl Acrylate. *J. Am. Chem. Soc.* **1998**, *120*, 888−899.
(55) Pollard, T. D.; Kellogg, D. A Guide to Simple and Informative Binding Assays. *Mol. Biol. Cell* **2010**, *21*, 4061−4067.
(56) We are aware, that the interpretation of the binding of weak ligands via the fluorescence method requires caution. A low concentration impurity might be characterized by stronger binding to the metal. However, in order to disturb the determination of the binding constant, the binding rate of the impurity has to be orders of magnitude higher than that of the weak ligand. Pyridine shows a much stronger affinity to the metal center than the olefins, but it is not characterized by massively faster binding.
(57) Chen, C. Redox-Controlled Polymerization and Copolymerization. *ACS Catal.* **2018**, *8*, 5506−5514.
(58) Allen, K. E.; Campos, J.; Daugulis, O.; Brookhart, M. Living Polymerization of Ethylene and Copolymerization of Ethylene/Methyl Acrylate Using "Sandwich" Diimine Palladium Catalysts. *ACS Catal.* **2015**, *5*, 456−464.
(59) Peschek, N.; Wannowius, K.-J.; Plenio, H. The Initiation Reaction of Hoveyda-Grubbs Complexes with Ethene. *ACS Catal.* **2019**, *9*, 951−959.
(60) O'Connor, K. S.; Lamb, J. R.; Vaidya, T.; Keresztes, I.; Klimovica, K.; LaPointe, A. M.; Daugulis, O.; Coates, G. W. Understanding the Insertion Pathways and Chain Walking Mechanisms of α-Diimine Nickel Catalysts for α-Olefin Polymerization: A ^{13}C NMR Spectroscopic Investigation. *Macromolecules* **2017**, *50*, 7010−7027.

DOI: 10.1021/acs.organomet.9b00130
Organometallics XXXX, XXX, XXX−XXX

(61) This is an approximate value, since the final solution in the cuvette contains ca. 50% (wt) of styrene.
(62) Chen, Z.; Liu, W.; Daugulis, O.; Brookhart, M. Mechanistic Studies of Pd(II)-Catalyzed Copolymerization of Ethylene and Vinylalkoxysilanes: Evidence for a β-Silyl Elimination Chain Transfer Mechanism. *J. Am. Chem. Soc.* **2016**, *138*, 16120−16129.
(63) Kurosawa, H.; Majima, T.; Asada, N. Synthesis, structures, stabilities, and reactions of cationic olefin complexes of palladium(II) containing the η^5-cyclopentadienyl ligand. *J. Am. Chem. Soc.* **1980**, *102*, 6996−7003.
(64) Fernandez, I. Preliminary DFT calculations on [Pd(py)(Me)-(**3**)]BArF lend additional support to the d-PEt mechanism. Personal Communication, **2018**.
(65) Shaw, B. L.; Thornton-Pett, M.; Vessey, J. D. Preparation of α-diazines and α-2-pyridylazines containing (1R)-(+)-camphor or (1R)-(-)-fenchone residues and their complexes with Group 6 metal carbonyls. *J. Chem. Soc., Dalton Trans.* **1994**, 3597−3606.

DOI: 10.1021/acs.organomet.9b00130
Organometallics XXXX, XXX, XXX−XXX